01 Jun 2022

Thermal and Electrical Properties of a High Entropy Carbide (Ta, Hf, Nb, Zr) at Elevated Temperatures

Evan C. Schwind

Michael J. Reece

Elinor Castle

William Fahrenholtz
Missouri University of Science and Technology, billf@mst.edu

et. al. For a complete list of authors, see https://scholarsmine.mst.edu/matsci_eng_facwork/2884

Recommended Citation

E. C. Schwind et al., "Thermal and Electrical Properties of a High Entropy Carbide (Ta, Hf, Nb, Zr) at Elevated Temperatures," *Journal of the American Ceramic Society*, vol. 105, no. 6, pp. 4426 - 4434, Wiley, Jun 2022.
The definitive version is available at https://doi.org/10.1111/jace.18400

Received: 22 June 2021 | Revised: 16 December 2021 | Accepted: 3 January 2022

DOI: 10.1111/jace.18400

Journal of the American Ceramic Society

RESEARCH ARTICLE

Thermal and electrical properties of a high entropy carbide (Ta, Hf, Nb, Zr) at elevated temperatures

Evan C. Schwind[1] | **Michael J. Reece**[2] | **Elinor Castle**[2] | **William G. Fahrenholtz**[1] | **Gregory E. Hilmas**[1]

[1]Department of Materials Science and Engineering, Missouri University of Science and Technology, Rolla, Missouri, USA

[2]School of Engineering and Materials Science, Queen Mary University of London, London, UK

Correspondence
Evan C. Schwind, Department of Materials Science and Engineering, Missouri University of Science and Technology, Rolla, MO 65409, USA.
Email: ecsg3f@umsystem.edu

Funding information
EPSRC Programme Grant XMAT, Grant/Award Number: EP/K008749/2; EPSRC,, Grant/Award Number: EP/K008749/2

Abstract

The thermal and electrical properties were measured for a high entropy carbide ceramic, consisting of (Hf, Ta, Zr, Nb)C. The ceramic was produced by spark plasma sintering a mixture of the monocarbides and had a relative density of more than 97.6%. The resulting ceramic was chemically homogeneous as a single-phase solid solution formed from the constituent carbides. The thermal diffusivity (0.045–0.087 cm^2/s) and heat capacity (0.23–0.44 J/g•K) were measured from room temperature up to 2000°C. The thermal conductivity increased from 10.7 W/m•K at room temperature to 39.9 W/m•K at 2000°C. The phonon and electron contributions to the thermal conductivity were investigated, which showed that the increase in thermal conductivity was predominantly due to the electron contribution, while the phonon contribution was independent of temperature. The electrical resistivity increased from 80.9 $\mu\Omega$•cm at room temperature to 114.1 $\mu\Omega$•cm at 800°C.

KEYWORDS
electrical properties, thermal properties, ultra-high temperature ceramics

1 | INTRODUCTION

Ultra-high temperature ceramics are a class of materials with melting temperatures greater than 3000°C.[1] Among these materials are several transition metal carbides and, of specific interest recently, high entropy carbides (HECs).[2–5] These materials have the potential to be used in extreme environments such as those associated with aerospace and nuclear applications. HECs have unusual properties including hardness, strength, and elastic modulus values that can be higher than predicted from the properties of the constituent monocarbides.[2]

While the interest in HECs is recent, the initial interest in high entropy materials started with high entropy alloys (HEAs).[6–9] Some of the first papers to mention HEAs were published in 2004 by Yeh et al.[6,10,11] These papers introduced the "high entropy" concept and defined HEAs as alloys composed of five or more principal elements in equimolar ratios, although later papers expanded the definition to consider nonequimolar concentrations.[12] Yeh et al. used Equation 1 as a way to describe the stabilizing effect of multiprincipal element materials, where N is the number of components present in equimolar amounts, and R is the ideal gas constant. As N increases, the entropy of mixing (ΔS_{mix}) also increases. This increase in entropy was proposed to stabilize single-phase solid solutions, and the effect increases as temperature increases as the overall Gibbs' free energy of a system includes the factor -TΔS. They explain that while HEAs and systems may be difficult to process, HEAs are stable due to the high mixing entropy brought about by multiple components.

$$\Delta S_{mix} = R\ln N \quad (1)$$

Interest in HEAs stems from advantageous properties that have been reported, including increased wear resistance,[13] strength, and hardness.[14] Along with the entropy stabilization effect, the term "cocktail effect" was applied to describe unexpected properties or effects caused by the mixing of multiple elements. In some cases, the cocktail effect can result in a property that is much greater than suggested based on the amounts of the constituents and their reported properties. For example, the hardness of some HEAs has been reported to be much greater than predicted by a linear rule of mixtures (ROMs) and the hardness values of the constituent metals.[15] Likewise, improved oxidation resistance has been reported for high entropy borides and HECs.[16,17]

Another defining characteristic of high entropy materials is lattice distortion, which has been reported in both HEAs and high entropy ceramics.[18,19] Lattice distortion is proposed to occur because of the different sizes of the elements that constitute these materials. Because of the size difference, both the unit cell and the individual bonds can be strained. This phenomenon can affect the thermal and electrical conductivities of materials due to increased phonon scattering caused by strained bonds.[19,20]

Several high entropy ceramic systems have been investigated.[21–24] These materials have the same defining characteristics as HEAs, including increased stability at elevated temperatures, lattice distortion, and the cocktail effect. The ability of these ceramics to form high entropy materials is due to the propensity for solid solution formation in these systems. Initial studies were conducted on HECs and nitrides as coatings.[25,26] This has since been expanded to bulk materials and multiple systems including oxides, diborides, and more.

Castle et al. were the first to report the synthesis of a bulk HEC, which was a (Ta, Hf, Zr, Nb)C ceramic produced by Spark Plasma Sintering (SPS) at 2300°C.[2] They showed that the hardness measured by nanoindentation was ~5 GPa greater than any of the individual carbide components. The high hardness was attributed to a cocktail effect solid solution strengthening, and, possibly, lattice distortion. Feng at al. reported synthesis and densification of an HEC at much lower temperatures (1600 and 1900°C, respectively) than had previously reported.[5,27] By taking advantage of nanoscale powders they were able to carbothermally reduce multiple oxide precursors into a dense single phase HEC. Recently Feng et al. measured the flexure strength of (Ta, Hf, Zr, Nb, Ti)C. They observed a strength of ~421 MPa at room temperature. This was maintained up to 1800°C, and then a drop in strength was observed up to 2300°C (~93 MPa), which was attributed to an increase in dislocation movement that was restricted at lower temperatures due to the random elements in the cation sublattice.[28]

Lattice distortion has also been shown to affect the thermal conductivity of high entropy ceramics. Liu et al. utilized modeling and experimental analysis to identify the effect of multicomponent thermoelectric materials on the phonon contribution to thermal conductivity.[29] They found that in multicomponent systems K_p is lowered as the number of components increases due to local "mass and strain fluctuations." Yan et al.[19] synthesized an HEC containing Hf, Zr, Ta, Nb, and Ti. They measured the thermal conductivity of this material at multiple temperatures below 100°C and determined the thermal conductivity at ~30°C to be ~5.5 W/ m•K. The thermal conductivity was lower than the thermal conductivity values reported for most of the constituents, except for NbC. The reduction in thermal conductivity was thought to be due to lattice strain and subsequently scattering of phonons. Similar thermal conductivity behavior has been reported for other HECs and ceramics.[30–32]

Rost et al. investigated the effect of carbon content on the electron and phonon contributions to the thermal conductivity of HEC thin films.[33] They found that substoichiometric films exhibited metallic behavior, and electrons played a large role in the thermal conductivity. As carbon is added into the system, the contribution of phonons to thermal conductivity increased. Rost et al. utilized the Wiedemann–Franz law to perform this analysis and thus measured the electrical resistivity, although they did not explicitly report these measurements. They did, however, mention measuring electrical resistivities that were higher than for "typical metal carbides" and HEAs, which agrees with other reports of higher electrical resistivity in HECs.[34]

The goal of this paper was to analyze the thermal conductivity of (Ta, Hf, Nb, Zr)C at elevated temperatures. This paper is the first report of thermal diffusivity, heat capacity, electrical resistivity, and thermal conductivity of (Ta, Hf, Nb, Zr)C at elevated temperatures.

2 | EXPERIMENTAL DETAILS

2.1 | Processing

The processing of the specimens used in this study is the same as that described in detail in Castle et al.[2] and is summarized here. Commercially available powders of TaC (HC Stark, <44 μm), HfC (HC Stark, ~45 μm), ZrC (American Elements, <149 μm), and NbC (American Elements, <10 μm) were weighed out in equimolar amounts. The powder mixture was then ball milled for 24 h at 200 rpm in tungsten (W) and carbon (C) pots containing SiC milling media (5:1 ball:powder mass ratio) in an argon atmosphere. The milling cycle included steps of 5 min of milling followed by 5 min of resting to reduce heating of the mixed

powders. In addition, stearic acid was used as a mixing aid. The powder was initially subjected to a pressureless degassing step at 1800°C in flowing argon in a spark plasma sintering machine (FCT HPD 25; FCT Systeme GmbH, Rauenstein, Germany), which removed any oxide phases. The powder was then loaded into a graphite die and sintered at 2300°C under a pressure of 40 MPa for 7 min.

A similar processing procedure to the one described above was applied to the tantalum and hafnium carbide powders to produce bulk tantalum carbide and hafnium carbide for comparison to the properties of the HEC. The TaC and HfC were densified to 97.6% and 98.7% of their theoretical densities, respectively.

2.2 | Characterization

The bulk density of the sintered HEC ceramics was measured using Archimedes method (modified American Society for Testing and Materials (ASTM) C373). Ceramics were placed in boiling water for >2 h and then held under vacuum while still submerged.

The microstructure and the chemical composition were investigated using scanning electron microscopy (SEM; FEI Helios NanoLab 600, FEI, Hillsboro, OR) and energy dispersive spectroscopy (EDS; Oxford EDS, Oxford Instruments, Abingdon, UK). SEM and EDS were performed using an accelerating voltage of 20.0 kV, a current of 11 nA, and a working distance of 6 mm. Prior to characterization, specimens were ground so that their sides were flat and parallel. The specimens were polished starting with a series of diamond abrasives to a final finish using 0.25 μm diamond paste.

X-ray diffraction (XRD; X'Pert Pro, PANalytical, Almelo, Netherlands) was used to perform phase and crystallographic analysis. The ceramic was crushed and passed through a #200 mesh sieve prior to characterization. Rutile was used as an internal standard for calculation of lattice parameters. XRD was performed using Cu-Kα radiation ($\lambda = 1.5406$) from 5 to 138 °2θ with a step size of 0.026 °2θ and an effective counting time of 172.89 s per step. X'Pert highscore software was used for phase analysis. The lattice parameters of the HEC were measured by Rietveld refinement (RIQAS software) of the XRD data. The lattice parameters (a) were used, along with the average molecular weight (M) of the constituents in Equation 2 to calculate the theoretical density. Four atoms per unit cell were assumed (z), and N_A is Avogadro's number.

$$\rho = \frac{M\ z}{a^3\ N_A} \tag{2}$$

Electrical resistivity was measured in a tube furnace (Lindberg Blue M HTF55322A, Asheville NC) using the 4-point van der Pauw method (ASTM F76) from room temperature to 800°C. The measured electrical resistivity exhibited a linear relationship with temperature, thus it was deemed acceptable to extrapolate the data to 1600°C. Measurements were made every 100°C on specimens that were ground flat and parallel. The specimens were equilibrated for ~10 min at each temperature prior to testing. All of the tests were conducted under flowing argon except for the ambient temperature measurements, which were conducted in air. Prior to the measurements, four annealed Inconel wires were attached to each of the specimens. Data were analyzed using the methodology described in ASTM F76 to calculate electrical resistivity.

Thermal diffusivity (D) and heat capacity (C_P) were measured using the laser flash method (ASTM E1461) from ambient temperatures to 200°C in intervals of 50°C (Cryo2000; Anter Corp., Pittsburgh, PA) and from 200 to 2000°C in intervals of 100°C (Flashline 5000; Anter Corp.). Specimens were right circular cylinders that were ~12 mm in diameter and 2–3 mm thick. The specimen faces were coated using graphite spray prior to testing to ensure uniform adsorption of the laser light. All of the tests were run in flowing argon. The thermal diffusivity was calculated using the Clark and Taylor method (ASTM E1461).[35] The temperature was monitored at each hold, and tests were not conducted until the measured temperature had stopped changing to ensure that thermal equilibrium had been reached.

Measured values of thermal diffusivity and heat capacity were combined with the temperature adjusted density (~4%–6% change in density from room temperature to 2000°C for constituent carbides) to calculate thermal conductivity (k) using Equation 3. The adjusted density values were approximated using the coefficient of thermal expansion data reported by Singh and Weidemeier.[36] The thermal conductivity was then corrected to account for the porosity present in the sample using the Maxwell equation where P is the volume fraction of porosity (Equation 4), and k_{por} is the corrected thermal conductivity.[37]

$$k = D\ \rho\ C_p \tag{3}$$

$$k_{por} = k\frac{(1 + 0.5P)}{(1 - P)} \tag{4}$$

The electron contribution to thermal conductivity was estimated using the Weidemann–Franz law[38] (Equation 5), where k_e is the electronic contribution to the thermal conductivity, σ is electrical conductivity, L is the Lorenz number, and T is absolute temperature.

TABLE 1 Lattice parameters of (Hf, Ta, Zr, Nb)C and its carbide constituents[40]

	TaC	NbC	HfC	ZrC	ROM	(Hf, Ta, Zr, Nb)C
Lattice parameter (Å)	4.455	4.475	4.639	4.694	4.566	4.559

Abbreviation: ROMs, rule of mixtures.

$$\frac{\kappa_e}{\sigma} LT \tag{5}$$

The phonon contribution to thermal conductivity (k_p) was estimated by subtraction using Equation 6.

$$k_e + k_p = k \tag{6}$$

The Lorentz number used for the calculations was estimated based on a calculated value. Using the theoretical Lorenz number ($L_0 = 2.44 \times 10^{-8}$ WΩK^{-2}) gave negative values for k_p. Based on these results, the Lorenz number was estimated to be 2.33×10^{-8} WΩK^{-2} by finding the smallest number that resulted in non-negative values for the phonon contributions at all temperatures. Previous studies have presented further justification for use of an experimentally determined Lorenz number compared to the theoretical value.[39]

3 | RESULTS AND DISCUSSION

3.1 | Microstructure/phase analysis

A single-phase (Hf, Ta, Zr, Nb)C ceramic was produced by the SPS process. Analysis of the XRD pattern (Figure 1) revealed the presence of a single cubic phase with the rock salt structure. This demonstrates that the processing conditions produced a single phase solid solution HEC.

The HEC was nearly fully dense. The bulk density measured by Archimedes method was 10.12 g/cm^3. The theoretical density for the HEC was estimated to be 10.37 g/cm^3 based on the lattice parameters obtained from XRD and the average molecular weight of the constituent metals. The different metals were assumed to be randomly distributed on the sites in the rock salt lattice for this calculation. Table 1 shows the lattice parameters calculated for the HEC compared to its constituents and the lattice parameter predicted by a linear ROMs.[40] Comparing the measured bulk density to the calculated theoretical density gives a relative density of ~97.6%.

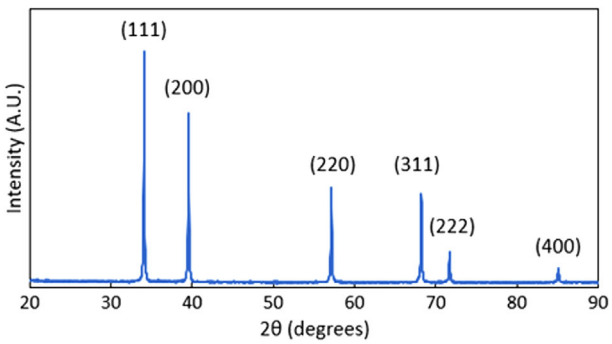

FIGURE 1 X-ray diffraction (XRD) pattern for (Hf, Ta, Zr, Nb)C indexed to the rock salt crystal structure

The HEC appeared to be chemically homogenous based on area EDS analysis (Figure 2) that indicated a uniform distribution of Hf, Ta, Zr, Nb, and C throughout the microstructure. Complementary SEM imaging (Image A) showed a uniform structure with an average grain size of 6.6 ± 3.6 μm (Feret diameter) and a porosity of ~0.24 vol% (assuming area% was equal to volume %). The density measured via Archimedes method, which was lower than the density estimated fromSEM image analysis, was considered more reliable because it measures the density of a bulk specimen as opposed to several small sections. The HEC was determined to be a single phase solid solution and appropriate for a detailed analysis of the intrinsic thermal and electrical properties based on its relative density, phase purity, and chemical homogeneity.

Multiple factors have been shown to affect the thermal and electrical properties of refractory metal carbides including point defects such as carbon vacancies and relative density (i.e., porosity). Williams studied the effect of vacancies on the electrical resistivity of some refractory metal carbides.[41] He noted that as the number of carbon vacancies in TiC and TaC increased, the electrical resistivity increased.[42] Williams noted that this is due to the ability of carbon vacancies to scatter conduction electrons. The electron scattering mechanism was confirmed through the residual resistivity exhibited by substoichiometric NbC, TaC, and HfC at low temperatures but not by fully stoichiometric WC. Storms and Paul investigated the thermal conductivity of ZrC and NbC as a function of carbon vacancy content.[43] They observed an increase in thermal conductivity as the number of carbon vacancies decreased, and the carbides approached a 1:1 carbon to metal stoichiometry. Yan et al. investigated the effect of porosity on the properties of ZrC, including thermal conductivity.[44] They showed that as porosity increased, the thermal conductivity decreased. The following sections contain data from the technical literature for the thermal and electrical properties of ZrC, NbC, HfC, and TaC. The values were taken from published reports; however, the values may not be

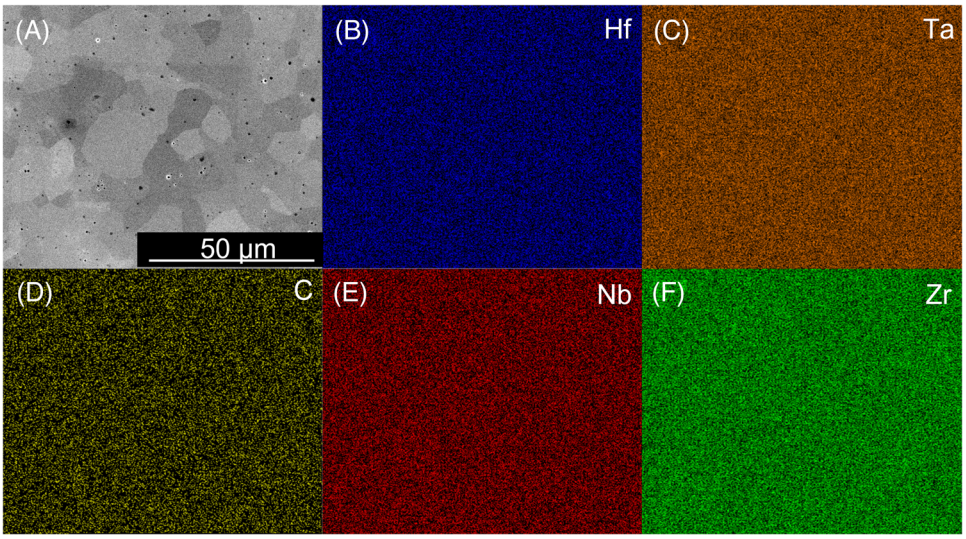

FIGURE 2 (Hf, Ta, Zr, Nb)C high entropy carbide showing (A) polished cross section, and energy dispersive spectroscopy (EDS) maps for (B) Hf, (C) Ta, (D) C, (E) Nb, and (F) Zr

the intrinsic values for these carbides due to a number of factors including variations in relative density and carbon stoichiometry. While some authors commented on these aspects of their specimens, others did not.

3.2 | Thermal diffusivity

The thermal diffusivity of the HEC increased from ~0.045 cm^2/s at 25°C to 0.087 cm^2/s at 2000°C. The thermal diffusivity of the HEC was ~27% lower than the average of the monocarbides across the entire temperature range measured. The measured diffusivity is significantly lower than the values for the individual carbides and the average predicted by a linear molar ROMs calculation (Figure 3). This phenomenon may be explained through the work of McClane et al. who showed that ZrB_2 containing 3 at% of transition metal solid solution additions had a lowered thermal diffusivity.[45,46] Each additional transition metal added into the HEC could act as further imperfections (i.e., acting as point defects similar to the vacancies mentioned above) in the lattice and lower the thermal diffusivity further. This is supported by Yan et al. who also reported the thermal diffusivity of a (Hf, Zr, Ta, Nb, Ti)C at ~30°C to be 0.036 cm^2/s.[19] This is lower than the diffusivity reported for (Hf, Ta, Zr, Nb)C in this work. The difference is most likely due to the addition of a 5th metallic element (Ti) into the HEC but may also be attributed to the lower density (93% of theoretical) of the HEC they measured. Yan et al. also showed that an ROMs was not followed and that the HEC had a lower thermal diffusivity than any of the components, similar to the results reported here.

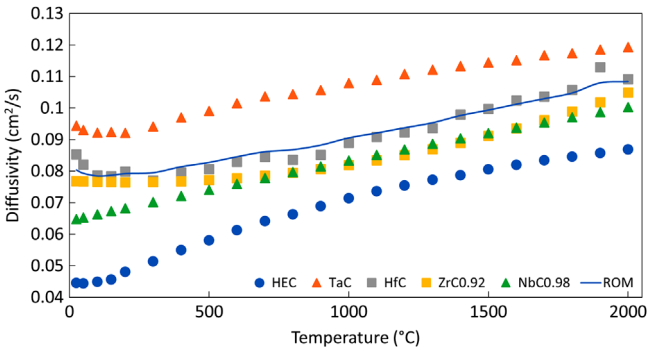

FIGURE 3 Thermal diffusivity of (Hf, Ta, Zr, Nb)C compared to TaC, and HfC (present work) and reported values for $ZrC_{0.92}$, $NbC_{0.98}$,[52] along with an average predicted by a molar rule of mixtures calculation

3.3 | Heat capacity

The heat capacity was measured for the HEC from room temperature up to 2000°C using the laser flash method (Figure 4) and was found to increase from ~0.23 J/g•K at 25°C to ~0.44 J/g•K at 2000°C. Reported heat capacities for TaC, ZrC, $NbC_{0.98}$,[47] and HfC,[48] along with an average value predicted by a linear molar ROMs calculation, are also included in Figure 4 for comparison to the HEC. The heat capacity of the HEC was similar to the value predicted by a linear molar ROMs calculation for the constituent monocarbides, differing by only about 2.4% across the entire temperature range investigated. Heat capacity scales with the mass of a material, so it would follow that the HEC has a heat capacity that is similar to

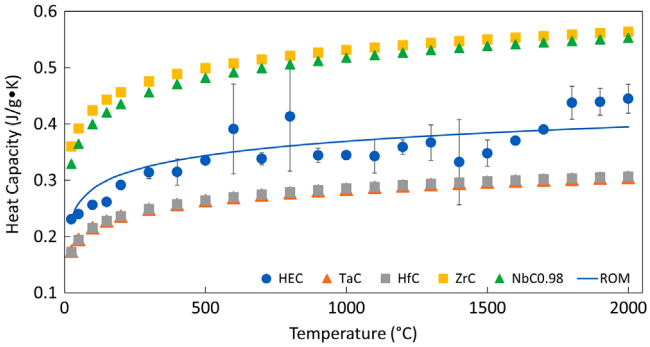

FIGURE 4 Heat capacity of (Hf, Ta, Zr, Nb)C compared to reported values for ZrC, $NbC_{0.98}$, TaC,[47] HfC[48] and the value predicted by a linear molar rule of mixtures

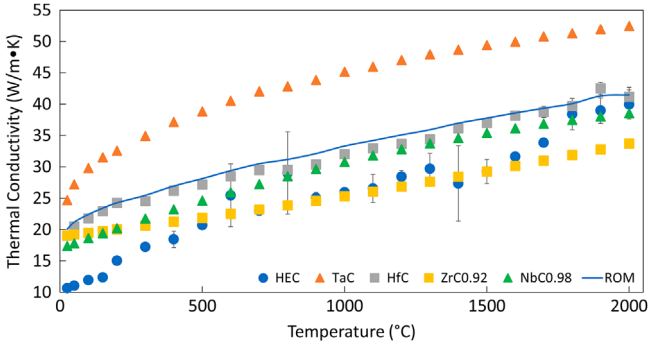

FIGURE 6 Thermal conductivity of the high entropy carbide (HEC) up to 2000°C compared to reported values for TaC, HfC (present work), ZrC, and NbC[52] along with an average value predicted by a linear molar rule of mixtures

the average of the individual carbides. This is the basis behind the Kopp–Neumann law that predicts the specific heat capacity of a compound.[49] The heat capacity of the HEC deviated from the average by ~12.3% at room temperature and ~0.54% at 2000°C. This observation, however, contradicts results reported by Yan et al.[19] who found that the heat capacity of their HEC was similar to the constituents with the lowest heat capacities.

3.4 | Electrical resistivity

The electrical resistivity of the HEC increased from 80.9 ± 0.1 μΩ•cm at 25°C to 114.1 ± 3.9 μΩ•cm at 800°C as shown in Figure 5. This was extrapolated to 1600°C (152.3 μΩ•cm) based on an assumed linear trend, which has been reported for the electrical resistivity of carbide ceramics.[50,51] The reported electrical resistivities for TaC, HfC (present work), and reported values for ZrC and NbC[50] along with an average electrical resistivity as a function of temperature, predicted by a linear molar ROMs

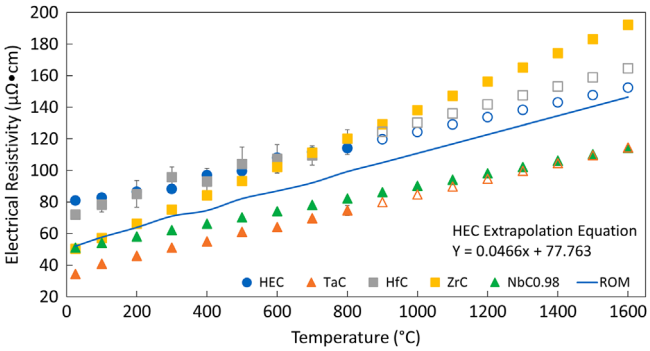

FIGURE 5 Electrical resistivity of high entropy carbide (HEC) measured from room temperature to 800°C (open data point is extrapolated to 1600°C) compared to TaC, HfC (present work), ZrC, and NbC[50]

calculation, are also included in Figure 5 for comparison to the HEC. The electrical resistivity of the HEC is lower than for HfC (~10.2% difference) and ZrC (~27% difference), but higher than the values for NbC (~45% difference), and TaC (~52.9% difference) across the temperature range investigated. The HEC does not follow an ROM for either thermal diffusivity or electrical resistivity as both thermal (Ke component of thermal conductivity) and electrical transport are influenced by electron transport. Elements of different atomic mass placed randomly throughout the crystal structure act as point scattering sources and may slow the movement of electrons, similar to carbon vacancies as studied by Williams.[41] The electrical resistivity does approach the average of the carbide constituents as temperature increases. This can be attributed to the resistivity of ZrC, which has a higher reported temperature coefficient (0.09 μΩ•cm/°C) than the other carbide materials (between 0.04 and 0.057 μΩ•cm/°C).

The electrical resistivity has only been reported for one other HEC ceramic, which had a composition of (Hf, Zr, Ta, Nb, Ti)C.[34] The resistivity was 91.3 μΩ•cm at room temperature (Table 2), which is higher than the value measured in the present study. The higher resistivity may be due to the additional metal element present in the ceramic in the previous study, but other factors such as porosity and carbon stoichiometry may contribute as well.

3.5 | Thermal conductivity

Figure 6 shows the thermal conductivity of the HEC compared to HfC, TaC (calculated from data gathered in this study), and $NbC_{0.98}$ and $ZrC_{0.92}$[52] along with the average value predicted using a linear molar ROMs calculation. The thermal conductivity of the HEC (10.7 W/m•K at room temperature and 39.9 ± 2.3 W/m•K at 2000°C) was noticeably lower than all of the constituent carbides except for

TABLE 2 Thermal conductivity and electrical resistivity of HEC materials[19,30,31,34,53]

Author	HEC	Thermal conductivity/temperature	Electrical resistivity/temperature
Yan et al.[19]	(Hf, Zr, TaTi, Nb)C	5.5 W/m•K, 30°C	N/A
Ye et al.[30]	(Zr, Nb, Ti, V)C	15.3 W/m•K, RT	N/A
Liu et al.[31]	(V, Nb, Ta, Mo, W)C	9.2 W/m•K, RT	N/A
Wei et al.[53]	(Ti, Zr, Hf, Nb, Ta)C	12.3 W/m•K, 50°C-19.2 W/m•K, 500°C	N/A
Ye et al.[34]	(Hf, Zr, Ta, Nb, Ti)C	N/A	91.3 $\mu\Omega$•cm, RT

Abbreviation: HEC, high entropy carbide; N/A, not available; RT, room temperature.

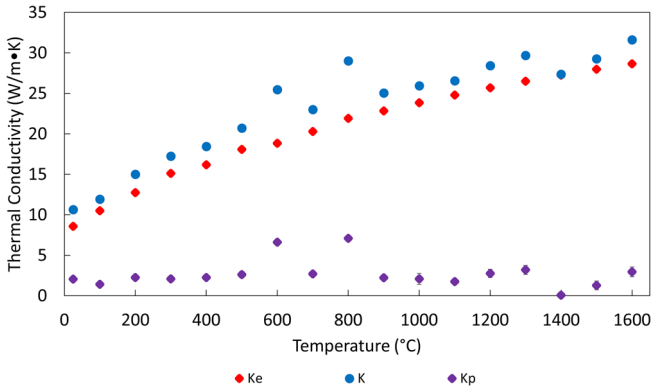

FIGURE 7 Thermal conductivity of the high entropy carbide (HEC), along with the phonon and electron contributions, up to 1600°C

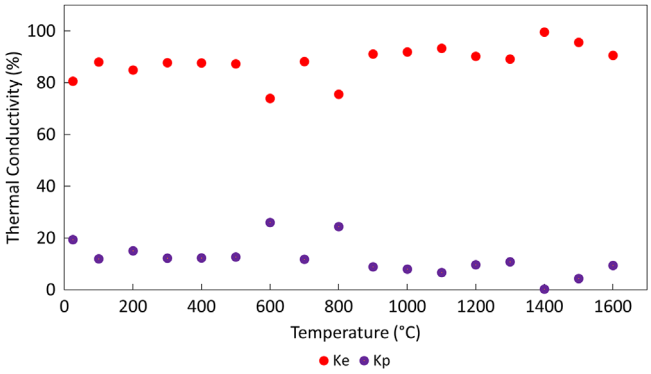

FIGURE 8 Phonon and electron contribution to thermal conductivity as percentage, up to 1600°C

$ZrC_{0.92}$, which had similar values, although the thermal conductivity was most likely lowered due to its substoichiometry. Presumably, the presence of metals, with different sizes and masses, disrupted phonon transport in the HEC,[46] causing decreases in both thermal diffusivity and thus thermal conductivity. The lattice strain described in previous reports of HECs could also contribute to the increased phonon scattering.[2]

A few reports measured the thermal conductivity of both four and five constituent HECs (Table 2).[19,30,31,53] The values indicate that more elements result in a lower thermal conductivity, although other factors such as porosity and carbon content may also affect the reported thermal conductivity.

To further analyze thermal transport, the phonon contribution to the thermal conductivity was estimated by subtracting the estimated electron contribution from the total thermal conductivity. The phonon contribution remained constant at ~2.7 W/m•K (this should be seen as a lower limit because K_P can vary depending on the value chosen for L) at all temperatures (Figure 7). Further, the phonon contribution was much lower than the electron contribution at all temperatures as shown in Figure 8. Interestingly, the increase in the electron contribution to thermal conductivity (8.6 W/m•K at 25°C to 28.7 W/m•K at 2000°C) led to an increase in thermal conductivity with temperature, similar to previous reports for rock salt carbides.[54–56] Hence, the thermal conductivity of HECs appears to be controlled by the same phenomena as for the constituent carbides (i.e., electron contribution). The thermal conductivity of the HEC was lower than the individual carbides due to lower phonon and electron contributions that result from the presence of multiple transition metal species with different ionic radii and mass.

4 | CONCLUSION

The thermal and electrical properties were studied for a (Hf, Ta, Zr, Nb)C ceramic. The HEC was a single-phase solid solution and was nearly fully dense. The thermal diffusivity (0.045–0.087 cm^2/s) was lower than all of the constituent carbides. The heat capacity of the HEC matched closely with the value obtained from an ROMs approximation from room temperature to 2000°C (~2.5% difference). The values for heat capacity were also higher than those of prior reports for HECs. The electrical resistivity (80.9 $\mu\Omega$•cm at 25°C to 114.1 $\mu\Omega$•cm at 800°C) of the HEC was higher than predicted by ROM.

The thermal conductivity of the HEC (10.7 W/m•K at 25°C and 39.9 W/m•K at 2000°C) was much lower than all of the individual carbide constituents (except $ZrC_{0.92}$, which was similar) and did not exhibit behavior

consistent with a linear ROMs.[52] This is most likely due to the presence of the metal atoms of differing ionic radii and mass causing scattering of phonons and electrons. The phonon contribution to the thermal conductivity was constant across the entire temperature regime tested at ~2.7 W/m•K, while the electron contribution increased from 8.6 W/m•K at room temperature to 28.7 W/m•K at 2000°C. This behavior is similar to that exhibited by other rock salt carbides in previous studies.

ACKNOWLEDGMENTS

This research was conducted as part of the Enabling Materials for Extreme Environments Signature Area at Missouri University of Science and Technology. The authors also acknowledge the use of the Advanced Materials Characterization Laboratory at Missouri S&T. The research was supported by the EPSRC Programme Grant XMAT (EP/K008749/2).

REFERENCES

1. Fahrenholtz WG, Hilmas GE, Talmy IG, Zaykoski JA. Refractory diborides of zirconium and hafnium. J Am Ceram Soc. 2007;90(5):1347–64.
2. Castle E, Csanádi T, Grasso S, Dusza J, Reece M. Processing and properties of high-entropy ultra-high temperature carbides. Sci Rep. 2018;8(1):1–12.
3. Sarker P, Harrington T, Toher C, Oses C, Samiee M, Maria JP, et al. High-entropy high-hardness metal carbides discovered by entropy descriptors. Nat Commun. 2018;9(1):1–10. http://doi.org/10.1038/s41467-018-07160-7
4. Harrington TJ, Gild J, Sarker P, Toher C, Rost CM, Dippo OF, et al. Phase stability and mechanical properties of novel high entropy transition metal carbides. Acta Mater. 2019;166:271–80. https://doi.org/10.1016/j.actamat.2018.12.054
5. Feng L, Fahrenholtz WG, Hilmas GE, Zhou Y. Synthesis of single-phase high-entropy carbide powders. Scr Mater. 2019;162:90–3. https://doi.org/10.1016/j.scriptamat.2018.10.049
6. Yeh JW, Chen SK, Lin SJ, Gan JY, Chin TS, Shun TT, et al. Nanostructured high-entropy alloys with multiple principal elements: novel alloy design concepts and outcomes. Adv Eng Mater. 2004;6(5):299–303.
7. Senkov ON, Wilks GB, Miracle DB, Chuang CP, Liaw PK. Refractory high-entropy alloys. Intermetallics 2010;18(9):1758–65. http://doi.org/10.1016/j.intermet.2010.05.014
8. Tsai KY, Tsai MH, Yeh JW. Sluggish diffusion in Co-Cr-Fe-Mn-Ni high-entropy alloys. Acta Mater. 2013;61(13):4887–97. http://doi.org/10.1016/j.actamat.2013.04.058
9. Cantor B, Chang ITH, Knight P, Vincent AJB. Microstructural development in equiatomic multicomponent alloys. Mater Sci Eng A. 2004;375–377:213–8. http://doi.org/10.1016/j.msea.2003.10.257
10. Miracle DB, Senkov ON. A critical review of high entropy alloys and related concepts. Acta Mater. 2017;122:448–511. http://doi.org/10.1016/j.actamat.2016.08.081
11. Yeh J, Chen S, Gan J, Lin S, Chin T. Communications: formation of simple crystal structures in Cu-Co-Ni-Cr-Al-Fe-Ti-V alloys with multiprincipal metallic elements. Metall Mater Trans A. 2010;35:2533–6.
12. Tsai MH, Yeh JW. High-entropy alloys: a critical review. Mater Res Lett. 2014;2(3):107–23. https://doi.org/10.1080/21663831.2014.912690
13. Chuang M, Tsai M, Wang W, Lin S, Yeh J. Microstructure and wear behavior of AlxCo1.5CrFeNi1.5Tiy high-entropy alloys Ming-Hao. Acta Mater. 2011;59:6308–17.
14. Senkov ON, Scott JM, Senkova S V, Miracle DB, Woodward CF. Microstructure and room temperature properties of a high-entropy TaNbHfZrTi alloy. J Alloys Compd. 2011;509(20):6043–8. http://doi.org/10.1016/j.jallcom.2011.02.171
15. Sanchez JM, Vicario I, Albizuri J, Guraya T, Garcia JC. Phase prediction, microstructure and high hardness of novel lightweight high entropy alloys. J Mater Res Technol. 2019;8(1):795–803. https://doi.org/10.1016/j.jmrt.2018.06.010
16. Gild J, Zhang Y, Harrington T, Jiang S, Hu T, Quinn MC, et al. High-entropy metal diborides: a new class of high-entropy materials and a new type of ultrahigh temperature ceramics. Sci Rep. 2016;6:2–11.
17. Wang Y, Reece MJ. Scripta materialia oxidation resistance of (Hf-Ta-Zr-Nb) C high entropy carbide powders compared with the component monocarbides and binary carbide powders. Scr Mater. 2021;193:86–90.
18. Lee C, Song G, Gao MC, Feng R, Chen P, Brechtl J, et al. Lattice distortion in a strong and ductile refractory high-entropy alloy. Acta Mater. 2018;160:158–72.
19. Yan X, Constantin L, Lu Y, Silvain JF, Nastasi M, Cui B. (Hf0.2Zr0.2Ta0.2Nb0.2Ti0.2)C high-entropy ceramics with low thermal conductivity. J Am Ceram Soc. 2018;101(10):4486–91.
20. Körmann F, Ikeda Y, Grabowski B, Sluiter MHF. Phonon broadening in high entropy alloys. npj Comput Mater. 2017;3(1):1–8. http://doi.org/10.1038/s41524-017-0037-8
21. Zhang R, Reece MJ. Review of high entropy ceramics: design, synthesis, structure and properties. J Mater Chem. 2019;7:22148–62.
22. Oses C, Toher C, Curtarolo S. High-entropy ceramics. Nat Rev Mater. 2020;5:295–309. http://doi.org/10.1038/s41578-019-0170-8
23. Backman L, Gild J, Luo J, Opila EJ. Acta materialia part I : theoretical predictions of preferential oxidation in refractory high entropy materials. Acta Mater. 2020;197:20–7. https://doi.org/10.1016/j.actamat.2020.07.003
24. Backman L, Gild J, Luo J, Opila EJ. Acta materialia part II : experimental verification of computationally pre dicte d preferential oxidation of refractory high entropy ultra-high temperature ceramics. Acta Mater. 2020;197:81–90. https://doi.org/10.1016/j.actamat.2020.07.004
25. Braic V, Vladescu A, Balaceanu M, Luculescu CR, Braic M. Surface & coatings technology nanostructured multi-element (TiZrNbHfTa) N and (TiZrNbHfTa) C hard coatings. Surf Coat Technol. 2012;211:117–21. http://doi.org/10.1016/j.surfcoat.2011.09.033
26. Hsieh M, Tsai M, Shen W, Yeh J. Surface & coatings technology structure and properties of two Al – Cr – Nb – Si – Ti high-entropy nitride coatings. Surf Coat Technol. 2013;221:118–23. http://doi.org/10.1016/j.surfcoat.2013.01.036
27. Feng L, Fahrenholtz WG, Hilmas GE. Low-temperature sintering of single-phase, high-entropy carbide ceramics. J Am Ceram Soc. 2019;102(12):7217–24.

28. Feng L, Chen W, Fahrenholtz WG, Hilmas GE. Strength of single-phase high-entropy carbide ceramics up to 2300°C. J Am Ceram Soc. 2021;104(1):419–27.
29. Liu R, Chen H, Zhao K, Qin Y, Jiang B, Zhang T. Entropy as a gene-like performance indicator promoting thermoelectric materials. Adv Mater. 2017;29(38):1–7.
30. Ye B, Wen T, Nguyen MC, Hao L, Wang C, Chu Y. First-principles study, fabrication and characterization of $(Zr_{0.25}Nb_{0.25}Ti_{0.25}V_{0.25})C$ high-entropy ceramics. Acta Mater. 2019;170:15–23. https://doi.org/10.1016/j.actamat.2019.03.021
31. Liu D, Zhang A, Jia J, Meng J, Su B. Phase evolution and properties of (VNbTaMoW)C high entropy carbide prepared by reaction synthesis. J Eur Ceram Soc. 2020;40:2746–51.
32. Gild J, Wright A, Quiambao-tomko K, Qin M, Tomko JA, Braun JL, et al. Thermal conductivity and hardness of three single-phase high-entropy metal diborides fabricated by boro-carbothermal reduction and spark plasma sintering. Ceram Int. 2020;46(5):6906–13. https://doi.org/10.1016/j.ceramint.2019.11.186
33. Rost CM, Borman T, Delower M, Lim M, Quiambao-tomko KF, Tomko JA, et al. Acta materialia electron and phonon thermal conductivity in high entropy carbides with variable carbon content. Acta Mater. 2020;196:231–9. https://doi.org/10.1016/j.actamat.2020.06.005
34. Ye B, Wen T, Kehan H, wang C, Chu Y. First - principles study, fabrication, and characterization of $(Hf_{0.2}Zr_{0.2}Ta_{0.2}Nb_{0.2}Ti_{0.2})C$. J Am Ceram Soc. 2019;102:4344–52.
35. Clark LM, Taylor RE. Radiation loss in the flash method for thermal diffusivity. J Appl Phys. 1975;46:714–9.
36. Singh M, Wiedemeier H. Estimation of thermal expansion behaviour of some refractory carbides and nitrides. J Mater Sci. 1997;2:5749–51.
37. Ondracek G. The porosity dependence of the thermal conductivity for nuclear fuels. J Nucl Mater. 1973;46:253–8.
38. Wiedemann G, Franz R. Ueber die wärme-leitungsfähigkeit der metalle. Ann Phys. 1853;165(8):497–531.
39. Harrington GJK, Hilmas GE, Fahrenholtz WG. Effect of carbon on the thermal and electrical transport properties of zirconium diboride. J Eur Ceram Soc. 2015;35(3):887–96. http://doi.org/10.1016/j.jeurceramsoc.2014.09.035
40. Nakamura K, Yashima M. Crystal structure of NaCl-type transition metal monocarbides MC (M = V, Ti, Nb, Ta, Hf, Zr), a neutron powder diffraction study. Mater Sci Eng B. 2008;148:69–72.
41. Williams WS. Electrical properties of hard materials. Int J Refract Met Hard Mater. 1999;17(1):21–6.
42. Santoro G. Variation of some properties of tantalum arbide with carbon content. Trans Am Institure Mining, Metall Pet Eng. 1963;227(6):1361–8.
43. Storms EK, Paul W. Thermal conductivity of sub-stoichiometric ZrC and NbC. High Temp Sci. 1973;5(6):454–62.
44. Yan N, Fu Q, Zhang Y, Li K, Xie W, Zhang J, et al. Preparation of pore-controllable zirconium carbide ceramics with tunable mechanical strength, thermal conductivity and sound absorption coefficient. Ceram Int. 2020;46:19609–16
45. Lonergan JM, McClane DL, Fahrenholtz WG, Hilmas GE. Thermal properties of Hf-Doped ZrB_2 ceramics. J Am Ceram Soc. 2015;98(9):2689–91. http://doi.wiley.com/10.1111/jace.13717
46. McClane DL, Fahrenholtz WG, Hilmas GE. Thermal properties of $(Zr, TM)B_2$ solid solutions with TM = Ta, Mo, Re, V, and Cr. J Am Ceram Soc. 2014;98(2):637–44.
47. Schwind EC, Hilmas GE, Fahrenholtz WG. Thermal properties and elastic constants of ζ-Ta_4C_{3-x}. J Am Ceram Soc. 2020;103:2986–90.
48. Barin I. Thermochemical data of pure substances. 3rd ed. Weinheim, New York: VCH Verlagsgesellschaft mbH, VCH Publishers, Inc.; 1995.
49. Leitner J, Voňka P, Sedmidubský D, Svoboda P. Application of Neumann-Kopp rule for the estimation of heat capacity of mixed oxides. Thermochim Acta. 2010;497(1–2):7–13.
50. Malt'seva LF, Lapshov YK, Marmer EN, Samsanov GV. High temperature heater of niobium and zirconium carbides. Poroshkovaya Metall. 1965;11(35):87–93.
51. Nino A, Hirabara T, Sugiyama S, Taimatsu H. Preparation and characterization of tantalum carbide (TaC) ceramics. Int J Refract Met Hard Mater. 2015;52:203–8. http://doi.org/10.1016/j.ijrmhm.2015.06.015
52. Morrison BH, Sturgess LI. The thermal diffusivity and conductivity of zirconium carbide and niobium carbide from 100 to 2,500 ° K. J Chem Inf Model. 1970;7(4):351–8.
53. Wei X, Liu J, Bao W, Qin Y, Li F, Liang Y. High-entropy carbide ceramics with refined microstructure and enhanced thermal conductivity by the addition of graphite. J Eur Ceram Soc. 2021;41:4747–54. https://doi.org/10.1016/j.jeurceramsoc.2021.03.053
54. Williams WS. High-temperature thermal conductivity of transition metal carbides and nitrides. J Am Ceram Soc. 1966;49(3):156–9.
55. Taylor RE, Morreale J. Thermal conductivity of titanium carbide, zirconium carbide, and titanium nitride at high temperatures. J Am Ceram Soc. 1964;47(2):69–73.
56. Cedillos-Barraza O, Grasso S, Nasiri NA, Jayaseelan DD, Reece MJ, Lee WE. Sintering behaviour, solid solution formation and characterisation of TaC, HfC and TaC-HfC fabricated by spark plasma sintering. J Eur Ceram Soc. 2016;36(7):1539–48. http://doi.org/10.1016/j.jeurceramsoc.2016.02.009

How to cite this article: Schwind E, Reece MJ, Castle E, Fahrenholtz WG, Hilmas GE. Thermal and electrical properties of a high entropy carbide (Ta, Hf, Nb, Zr) at elevated temperatures. J Am Ceram Soc. 2022;105:4426–4434. https://doi.org/10.1111/jace.18400